EARTH SURFACE PROCESSES AND LANDFORMS
Earth Surf. Process. Landforms (2014)

Published online in Wiley Online Library
(wileyonlinelibrary.com) DOI: 10.1002/esp.3554

Integrating climate and local factors for geomorphological distribution models

Juha Aalto* and Miska Luoto
Department of Geosciences and Geography, University of Helsinki, Helsinki, Finland

Received 8 November 2013; Revised 12 February 2014; Accepted 17 February 2014

*Correspondence to: Juha Aalto, Department of Geosciences and Geography, University of Helsinki, BOX 64, Gustaf Hällströmin katu 2 a, 00014 Helsinki, Finland. E-mail: juha.aalto@helsinki.fi

ESPL
Earth Surface Processes and Landforms

ABSTRACT: Earth surface processes (ESPs) drive landscape development and ecosystem processes in high-latitude regions by creating spatially heterogeneous abiotic and biotic conditions. Ongoing global change may potentially alter the activity of ESPs through feedback on ground conditions, vegetation and the carbon cycle. Consequently, accurate modeling of ESPs is important for improving understanding of the current and future distributions of these processes. The aims of this study were to: (1) integrate climate and multiple local predictors to develop realistic ensemble models for the four key ESPs occurring at high latitudes (slope processes, cryoturbation, nivation and palsa mires) based on the outputs of 10 modern statistical techniques; (2) test whether models of ESPs are improved by incorporating topography, soil and vegetation predictors to climate-only models; (3) examine the relative importance of these variables in a multivariate setting. Overall, the models showed high transferability with the mean area under curve of a receiver operating characteristics (AUC) ranging from 0.83 to 0.96 and true skill statistics (TSS) from 0.52 to 0.87 for the most complex models. Even though the analyses highlighted the importance of the climate variables as the most influential predictors, three out of four models benefitted from the inclusion of local predictors. We conclude that disregarding local topography and soil conditions in spatial models of ESPs may cause a significant source of error in geomorphological distribution models. Copyright © 2014 John Wiley & Sons, Ltd.

KEYWORDS: earth surface processes; high-latitude environments; ensemble methods; peri-glacial geomorphology; spatial modeling

Introduction

Earth surface processes (ESPs) drive landscape development (Washburn, 1979; Ballantyne and Benn, 1994; French, 2007) and ecosystem processes (Fox, 1981; Walker, 1995; Malanson *et al.*, 2012) in high-latitude regions by creating spatially heterogeneous landforms and abiotic as well as biotic conditions (Burnett *et al.*, 1998; Virtanen *et al.*, 2010; le Roux and Luoto, 2014). Geomorphological distribution models (GDMs) are widely used to link spatial observations of ESPs with multiple environmental predictors simultaneously, utilizing a wide range of statistical modeling techniques (Walsh *et al.*, 1998; Dai and Lee, 2002; Luoto and Seppälä, 2002; Brenning and Azócar, 2010). However, GDMs are often based only on coarse-scaled climatic variables (i.e. climate envelope models; see e.g. Luoto and Hjort, 2004; Fronzek *et al.*, 2006, 2011), or solely on topographical and land cover data (e.g. Brenning *et al.*, 2007; Hjort and Luoto, 2008), thus failing to consider the potentially important factors operating concurrently or the optimal resolution of the input data (e.g. Hjort *et al.*, 2010; Etzelmüller, 2013; Potter, 2013).

Various levels of hierarchy exist in geomorphic process–environment relationships (Albrecht and Car, 1999). At the broader spatial scale (from 10 km^2 to 1000 km^2), climate has found to be strongly linked to the occurrence of ESPs thus establishing more general distribution patterns (e.g. Luoto *et al.*, 2004; Fronzek *et al.*, 2006). However, at finer spatial scales (from 0.01 km^2 to 10 km^2) other environmental conditions, for example topography, soil properties and vegetation, become relevant (Hjort and Luoto, 2009) (Figure 1). Indeed, accounting for all the key predictors is essential for capturing the correct process–environment relationships and obtaining realistic predictions of ESPs in time and space. Modern statistics (e.g. Breiman, 2001; Venables and Ripley, 2002; Luoto and Hjort, 2005; Elith *et al.*, 2008) provide flexible methods for studying complex relationships between ESPs and environmental predictors, connections that are often accompanied by non-linearities and threshold behavior (Schumm, 1979; Phillips, 2003; Hjort and Luoto, 2010; Goetz *et al.*, 2012). This methodology combined with spatial data provides effective tools for modeling ESPs in various environments across spatial scales (Walsh *et al.*, 1998; Hjort and Luoto, 2013), as demonstrated by previous studies e.g. Marmion *et al.* (2008), Hjort and Marmion (2009), and Ridefelt *et al.* (2010). However, the choice of data sets, different modeling techniques and the theories and assumptions underlying them can cause uncertainty in model predictions (Walsh *et al.*, 1998; Guisan and Zimmermann, 2000). In order to decrease prediction uncertainty, studies integrating data characterizing environmental variation at different spatial scales and model ensembles (i.e. combined prediction based on multiple model outputs) are needed to improve

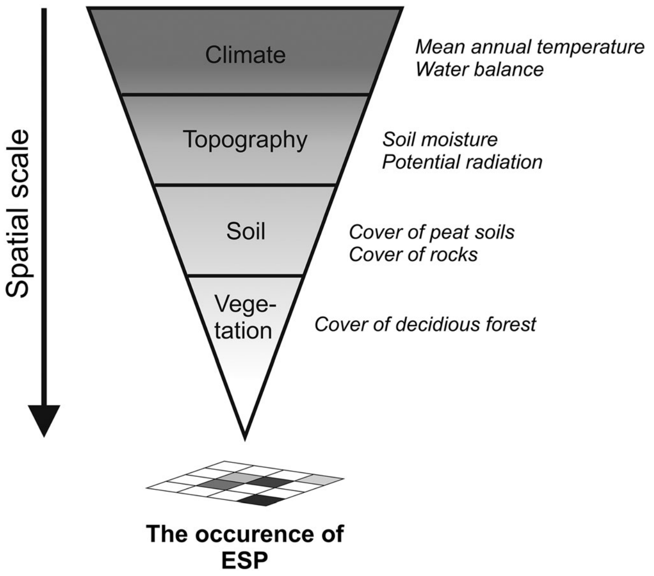

Figure 1. A conceptual model of the environmental factors and potential predictors determining the occurrence of earth surface processes (ESPs) across spatial scales.

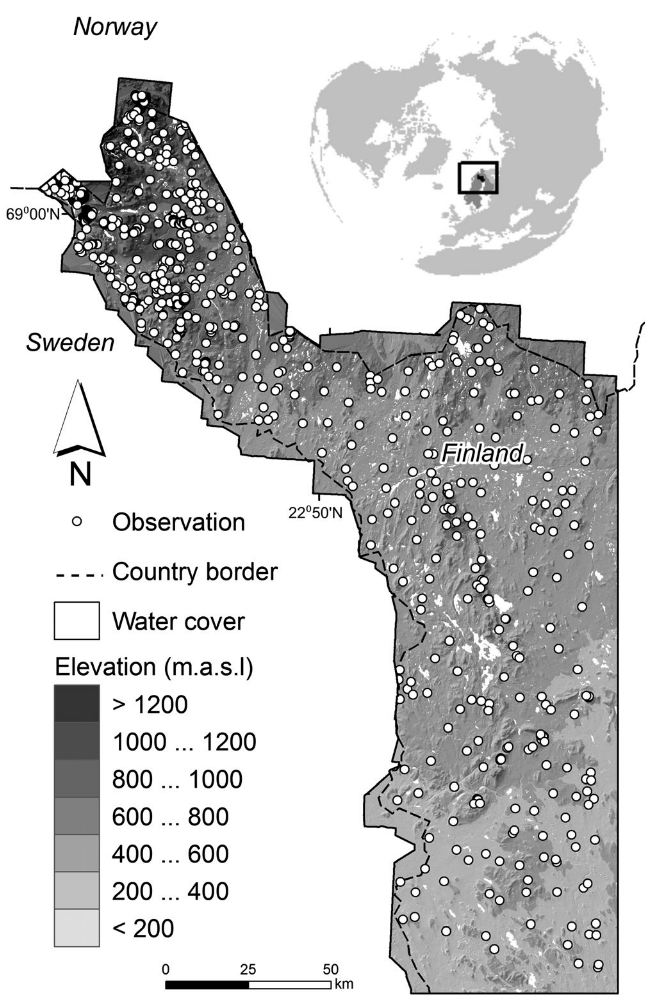

Figure 2. The location and topography of the study area in north-western Fennoscandia.

the accuracy of predictive models in geomorphology (Marmion *et al.*, 2009; Luoto *et al.*, 2010).

The predicted rise in temperatures by the end of this century will potentially have dramatic effects on topsoil temperature and moisture patterns, especially in high-latitude regions (IPCC, 2007). It can be postulated that this will alter the occurrence and intensity of ESPs (Etzelmüller *et al.*, 2011; Knight and Harrison, 2012; Farbrot *et al.*, 2013) with a direct linkage to a change in high-latitude ecosystems (Virtanen *et al.*, 2010; le Roux *et al.*, 2013a; le Roux *et al.*, 2013b) and geochemical cycles (Christensen *et al.*, 2004; Tarnocai *et al.*, 2009). Therefore, in order to understand the potential effects of climate change in high-latitude environments, the occurrences of ESPs in current climate conditions need to be correctly modeled (i.e. model predictions match the observed patterns). Hence, the aims of this study are: (1) to integrate climate and multiple local predictors to develop spatial models for four key ESPs occurring at high latitudes (slope processes, cryoturbation, nivation and palsa mires) based on an ensemble of 10 modern statistical modeling techniques; (2) to test whether the models of ESPs are improved by incorporating topography, soil and vegetation predictors to climate-only models; (3) to examine the relative importance of these variables in a multivariate setting. To achieve this, we used a comprehensive empirical data from northernmost Europe, modeled climate predictors as well as modern spatial modeling techniques.

Study Area

The study area covers *c.* 20 000 km^2 mainly in north-western Finland (including minor parts from Norway and Sweden; Figure 2). In this part of Fennoscandia, sub-arctic climate conditions prevail: mean July temperature (average of 1981 to 2010) varies from 12.6 °C to 1.3 °C, and the mean annual precipitation varies from 593 mm to 423 mm across the study area, with notable meso-scale variation depending on topographical position and proximity to the Arctic Ocean (Aalto *et al.*, 2014). Given the long-term development of the bedrock (0.4–3 Ga), topography also varies throughout the study domain with the highest fell tops located in the geologically younger regions of the study area of Caledonian rocks. The middle and southern parts consist of eroded Precambrian bedrock with gently sloping landscape (Laitakari, 1998). The study area is mainly covered by glacigenic till deposits, peat soils (formed in topographical depressions) and bare rock (fell areas), but sandy esker formations from Weichselian glaciations are also widespread. Vegetation shifts from spruce and Scots pine dominated forests in the south to mountain birch in the north of the study area (Sormunen *et al.*, 2010). Alpine vegetation, above the tree line, is characterized by shrubs and dwarf-shrubs.

Data and Methods

Earth surface processes

The geomorphological dataset used in this study consists total of 1150 study sites (25 m × 25 m in size) and includes the four main active ESP types occurring in the area. (1) Slow slope processes (i.e. solifluction) (Figure 3A) acting in high-latitudes are driven by gravity combined with freeze–thaw cycles of the active layer (Matsuoka, 2005; French, 2007). These mass movements produce various geomorphic features such as lobes, steps and stripes (Matsuoka, 2001; Harris *et al.*, 2008). (2) Cryoturbation (Figure 3B) is a general term for all upward and outward movement of the soil through frost action, creating features like patterned ground and earth hummocks (Washburn, 1979; Seppälä, 2005; French, 2007). In this study, cryoturbation was classified based on the dominant process

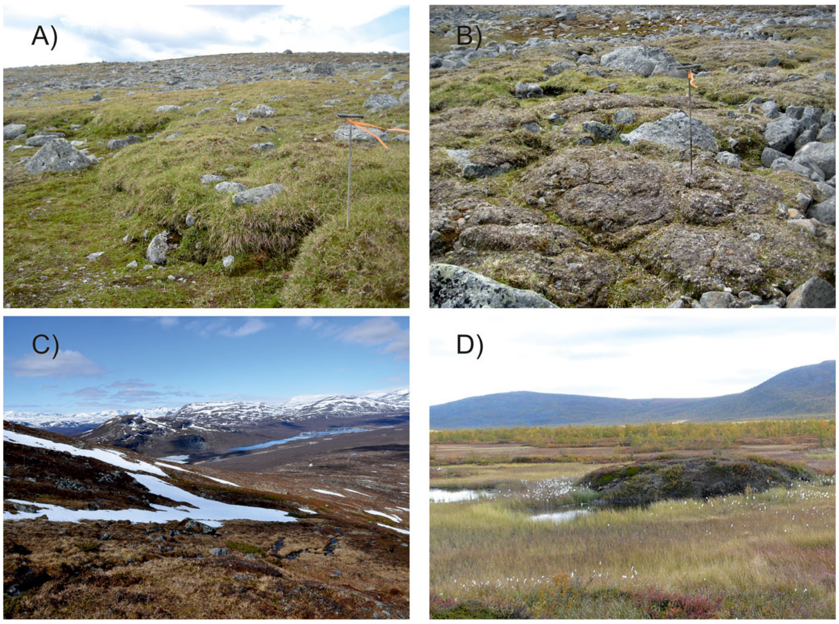

Figure 3. The main earth surface processes (ESPs) in the study area. (A) Slope processes [solifluction, 20°59′E 68°59′N, *c.* 810 m above sea level (a.s.l)], (B) cryoturbation (21°4′E 68°59′N, *c.* 880 m a.s.l), (C) nivation (local snow accumulation site, 20°48′E 69°3′N, *c.* 750 m a.s.l) and (D) palsa mire (21°25′E 68°43′N, *c.* 408 m a.s.l). This figure is available in colour online at wileyonlinelibrary.com/journal/espl

type, since these typically coexist with slope processes (Hjort and Luoto, 2010). Therefore, cryoturbation included sorted and non-sorted patterned ground as well as earth hummocks. (3) Nivation (Figure 3C) represents local snow accumulation sites related to multiple other hillslope processes e.g. weathering and fluvial processes (Thorn, 1979; Washburn, 1979; French, 2007). (4) Palsa mires (Figure 3D), mire complexes with a permanently frozen peat and a mineral sediment core, are characteristic features of peri-glacial landscapes, representing the outer margin of the discontinuous permafrost zone (Seppälä, 1988, Luoto *et al.*, 2004).

Aerial photography (spatial resolution of 0.25 m^2; Land Survey of Finland, 2013) and field investigations based on visual analysis were used for the compilation of the geomorphological dataset (following the methodology in Hjort and Luoto, 2009). The sampling covered the whole study domain and main climatological and environmental gradients. A random sampling approach was not practical in this study, because of the extensive size of the study area and impassable wetlands. The activity/inactivity of the ESPs was determined based on the evidence in ground surface, indicated by e.g. frost-heaving, cracking, soil displacement and changes in vegetation cover. The process was considered active if even a small area of the process had some indicator of activity. A binary variable (1 = presence, 0 = absence) of each of the ESPs was established indicating only the evident activity (or absence) of ESPs.

Environmental predictors

The environmental predictor set included variables of climate, topography, soil and vegetation (Table I; Figure 4). Climatological conditions strongly influence the occurrence of ESPs at broader spatial scales (> 1 km^2) (e.g. Luoto *et al.*, 2004; Fronzek *et al.*, 2006). Monthly climatological averages (1981–2010) were modeled across the study area (at the spatial resolution of 200 m × 200 m) based on generalized additive modeling utilizing variables of geographical location, topography and water cover. The climate dataset comprises of 61 meteorological stations covering the northern parts of Fennoscandia from the national observation networks of Finland, Sweden and Norway (Aalto *et al.*, 2014). Subsequently, four explanatory variables with known correlation to

Table I. The description of the environmental predictors used in this study with mean, minimum (Min) and maximum (Max) values shown

Category	Variable	Description	Unit	Mean	Min	Max
Climate	TMEAN	Mean annual temperature (1981–2010)	°C	−2.2	−4.5	0.5
	TDD	Thawing degree days (accumulated daily temperature sum above 0 °C)	°C	969	366	1560
	FDD	Freezing degree days (accumulated daily temperature sum below 0 °C)	°C	−1714	−2082	−1478
	WAB	Water balance (the difference between annual precipitation sum and potential evaporation)	mm	346	225	506
Topography	Slope	Slope angle	Degree	9	0	45
	TWI	Topographical wetness index	index	4.6	0.5	22.0
	Radiation	Potential annual direct radiation	MJ/cm^2/a	0.42	0.19	0.80
	Curvature	Concavity/convexity of the surface	index	0.02	−1.76	3.36
Soil	Peat	Cover of peat soils	%	13	0	100
	Rock	Cover of rocks	%	46	0	100
	Sand	Cover of sandy soils	%	3	0	100
Vegetation	Coniferous	Cover of coniferous forest	%	10	0	100
	Deciduous	Cover of deciduous forest	%	17	0	100

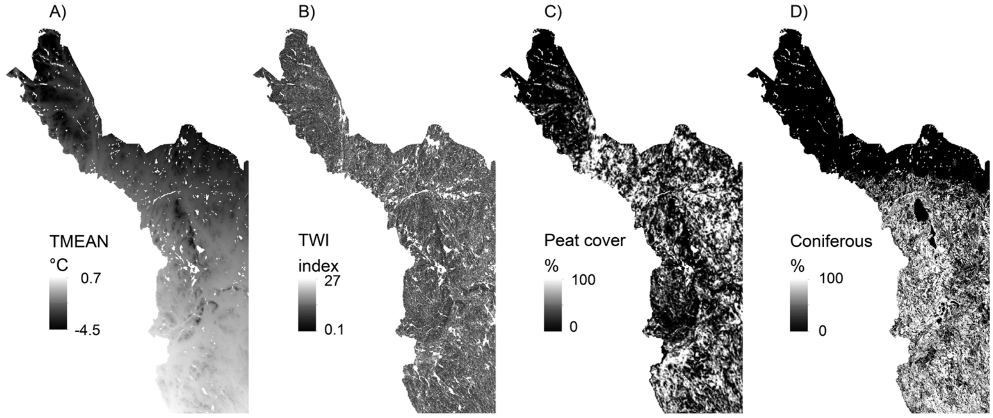

Figure 4. Examples of the environmental predictors used for modeling ESPs across the study area at the spatial resolution of 200 m × 200 m (water cover is excluded). (A) Mean annual temperature (TMEAN) 1981–2010 (in °C), (B) topographical wetness index (TWI), (C) cover of peat (%) and (D) cover of coniferous forest (%).

the occurrences of ESPs were derived from the modeled climate dataset (see e.g. Fronzek *et al.*, 2006): annual mean temperature (TMEAN) (Figure 4A), freezing degree days (FDD), thawing degree days (TDD) and water balance (WAB). TDD and FDD are based on the effective temperature sum of mean daily temperatures above or below 0 °C, respectively (Carter *et al.*, 1991; Fronzek *et al.*, 2006). WAB was determined as the difference between mean annual precipitation sum and potential evaporation (Skov and Svenning, 2004).

Topography is a major determinant of the variation in local slope stability, radiation and hydrological conditions. In our analyses we used four topography related variables derived from a digital elevation model (DEM; spatial resolution of 25 m × 25 m; Land Survey of Finland, 2013). These included slope angle (e.g. mass movement potential), topographical wetness index (TWI; e.g. soil moisture; Beven and Kirkby, 1979) (Figure 4B), potential annual direct solar radiation (MJ/cm^2/a; temperature conditions of the surface) and total curvature (e.g. snow conditions; positive value indicating ridge tops and negative values valley bottoms). Slope angle and total curvature were calculated with the *Spatial analyst* extension in ArcGis 10.0. TWI was calculated using *Python* script written by Prasad Pathak (Esri, 2013), whereas potential annual solar radiation (McCune and Keon, 2002) was calculated using ArcView 3.2 *Solar analyst* extension accounting for latitude, slope angle and slope aspect.

Soil variables are related to the occurrence of ESPs through the thermal and hydrological properties of soil (French, 2007). The three soil predictors were peat cover (high moisture content, low thermal conductivity) (Figure 4C), bare rock (low moisture content, high thermal conductivity) and sand cover (frost resistant, low moisture content). The soil classes were reclassified from a digital soil database (Geological Survey of Finland, 2010; spatial resolution of 20 m × 20 m) and the created binary masks were transformed to a continuous scale using mean filter with window size of 100 m × 100 m (ArcGis 10.0 *focal mean* function).

Vegetation has a clear influence on the distribution of snow, soil moisture and soil temperature as well as gravitational processes with generally negative effects on the cryogenic activity (e.g. Washburn, 1979; Hjort and Luoto, 2009). Therefore, we included two vegetation variables in the analysis: cover of coniferous forest (%) (Figure 4D) and cover of deciduous forest (%). Vegetation data was compiled from the Corine 2006 land cover dataset with a spatial resolution of 25 m × 25 m (Finnish Environmental Institute, 2006). To obtain spatial predictions across the study area, the predictors described were resampled to 200 m × 200 m resolution by spatial averaging (ArcGis 10.0 *Zonal Statistics* function). In Table II the occurrences of ESPs in relation to predictors are presented.

Statistical modeling

The observations of ESPs were related to predictors (resolution of 25 m × 25 m) by using 10 state-of-the-art statistical modeling techniques: generalized linear modeling (GLM; McCullagh and Nelder, 1989), generalized additive modeling (GAM; Hastie and Tibshirani, 1990), artificial neural networks (ANN; Venables and Ripley, 2002), classification tree analysis (CTA; Breiman *et al.*, 1984), generalized boosting methods (GBM; Elith *et al.*, 2008), random forest (RF; Breiman, 2001), multiple adaptive regression splines (MARS; Friedman, 1991), surface range envelope (SRE; Beamount *et al.*, 2005), flexible discriminant analysis (FDA; Hastie *et al.*, 1994) and maximum entropy (MAXENT; Phillips *et al.*, 2006). More detailed information on the techniques utilized and their parameters is provided as Supplementary Material Appendix A. All the modeling methods are implemented in the *Biomod2* platform (Thuiller *et al.*, 2013) under *R*-program (R Development Core Team, 2011).

The models of ESPs were fitted using four sets of predictors: (1) climate only; (2) climate and topography; (3) climate, topography and soil; (4) climate, topography, soil and vegetation:

Occurrence of ESPs = TMEAN + TDD + FDD + WAB
[Climate-only model, CM]

Occurrence of ESPs = CM + Radiation + Slope angle + Curvature + TWI
[Climate–topography model, CTM]

Occurrence of ESPs = CTM + Rock cover + Sand cover + Peat cover
[Climate–topography–soil model, CTSM]

Occurrence of ESPs = CTSM + Cover of coniferous forest + Cover of deciduous forest
[Full model]

The transferability (i.e. generality) of the model combinations were assessed by using four-fold cross-validation (i.e. the models were fitted using 70% of the data and evaluated against the remaining 30%). We compared the predicted and observed occurrences of ESPs by calculating the area under the curve of a receiver operating characteristic (AUC) plot and true skill statistics (TSS) based on four evaluation runs. AUC is a threshold-independent measure of predictive accuracy assessing

Table II. The occurrence of earth surface processes (ESPs) in relation to the mean and standard deviation (±) values of predictors utilized in the analysis

ESP		*n*	TMEAN	TDD	FDD	WAB
Slope processes	1	374	–2.8 (± 0.7) ***	788 (± 187) ***	–1723 (± 99) *	397 (± 65) ***
	0	776	–1.9 (± 0.8)	1056 (± 213)	–1709 (± 135)	321 (± 62)
Cryoturbation	1	309	–2.9 (± 0.6) ***	756 (± 179) ***	–1733 (± 98)***	399 (± 67) ***
	0	841	–1.9 (± 0.8)	1047 (± 211)	–1707 (± 132)	327 (± 64)
Nivation	1	153	–3.0 (± 0.6) ***	703 ± (172) ***	–1705 (± 87) n.s.	428 (± 56) ***
	0	997	–2.0 (± 0.8)	1009 (± 223)	–1715 (± 129)	334 (± 66)
Palsa mires	1	134	–2.0 (± 0.4) ***	1053 (± 111) ***	–1779 (± 122) ***	295 (± 35) ***
	0	1016	–2.2 (± 0.9)	957 (± 251)	–1705 (± 122)	353 (± 73)
			Slope	Radiation	Curvature	TWI
Slope processes	1		16 (± 8.8) ***	0.434 (± 0.13) *	0.02 (± 0.6) n.s.	3.5 (± 1.4) ***
	0		6 (± 6.5)	0.426 (± 0.1)	0.02 (± 0.4)	5.1 (± 2.6)
Cryoturbation	1		11 (± 9.2) ***	0.401 (± 0.1) ***	–0.03 (± 0.5) ***	4.3 (± 1.9) n.s.
	0		8.6 (± 8.4)	0.439 (± 0.1)	0.04 (± 0.4)	4.7 (± 2.5)
Nivation	1		16 (± 7.4) ***	0.370 (± 0.1) ***	–0.13 (± 0.6) ***	3.9 (± 1.5) ***
	0		8.1 (± 8.3)	0.437 (± 0.1)	0.05 (± 0.4)	4.7 (± 2.5)
Palsa mires	1		0.7 (± 0.7) ***	0.418 (± 0.01) n.s.	0.01 (± 0.2) n.s.	7.9 (± 3.1) ***
	0		10.3 (± 8.6)	0.430 (± 0.1)	0.02 (± 0.5)	4.1 (± 1.9)
			Sand	Rock	Peat	
Slope processes	1		0.07 (± 0.9) ***	81.6 (± 28.8) ***	0.25 (± 1.1) ***	
	0		4.3 (± 12.8)	28.4 (± 36.9)	18.8 (± 28.0)	
Cryoturbation	1		0.28 (± 2.1) ***	66.3 (± 40.5) ***	3.3 (± 12.0) ***	
	0		3.8 (± 12.8)	38.1 (± 40.8)	16.3 (± 27.0)	
Nivation	1		0.04 (± 0.4) ***	86.4 (± 26.3) ***	0.1 (± 0.7) ***	
	0		3.3 (± 11.5)	39.4 (± 41.1)	14.7 (± 25.9)	
Palsa mires	1		4.0 (± 11.6) n.s.	4.5 (± 12.2) ***	55.5 (± 25.3) ***	
	0		2.8 (± 10.6)	51.1 (± 42.2)	7.2 (± 18.2)	
			Coniferous	Deciduous		
Slope processes	1		0.01 (± 0.05) ***	0.03 (± 0.1) ***		
	0		0.14 (± 0.33)	0.24 (± 0.4)		
Cryoturbation	1		0 ± (0) ***	0.01 (± 0.1) ***		
	0		0.13 (± 0.3)	0.23 (± 0.4)		
Nivation	1		0 (± 0) ***	0.002 (± 0) ***		
	0		0.11 (± 0.3)	0.19 (± 0.3)		
Palsa mires	1		0 (± 0) ***	0.03 (± 0.1) ***		
	0		0.1 (± 0.3)	0.2 (± 0.3)		

The statistical significance of the differences between presence and absence of the ESPs is tested using Wilcoxon's related sample test and is indicated as: $^{***}p \leq 0.001$; $^{*}p \leq 0.05$; n.s. = not significant.

the agreement between the observed presence/absence values and model predictions (Fielding and Bell, 1997). The AUC values range from zero to one; a model providing excellent transferability has AUC higher than 0.9 and a fair model has an AUC ranging from 0.7 to 0.9 (see Swets, 1988). TSS is an accuracy measure that takes into account sensitivity (true positive rate) and specificity (true negative rate) and that is not sensitive to prevalence (i.e. the frequency of occurrence) (Equation 1):

$$\text{TSS} = \text{sensitivity} + \text{specificity} - 1 \tag{1}$$

TSS ranges from −1 to 1, where 1 indicates perfect agreement, 0 random performance and −1 perfect disagreement (Allouche *et al.*, 2006). The potential improvement of AUC and TSS values (i.e. the average of four cross-validation rounds) between the climate-only and full models over the 10 modeling techniques was tested using Wilcoxon's related sample test ($n = 10$).

The probabilities of the ESPs occurrence were predicted across the study area (at the spatial resolution of 200 m × 200 m) and converted to binary presence–absence predictions based on TSS values calculated based on cross-validation statistics. In order to investigate the effects of intermodal variability and to produce the final prediction maps, we fitted an ensemble of forecasts using a majority vote approach (Araújo and New, 2006; Gallien *et al.*, 2012). This technique combines the binary predictions of the utilized modeling algorithms (with different level of performance under different circumstances) to a single ensemble binary map. In this study, if six out of the 10 modeling techniques vote (i.e. predicts) occurrence of ESPs inside a cell, then presence to final output map in that given location is set (subsequently, number of votes less than six equals absence).

The contribution of a single predictor in the full model (i.e. all predictors included) was determined by calculating variable importance based on 50 permutation runs (Thuiller *et al.*, 2009). This high number of repeats was chosen because of potentially large sampling variability. In Biomod2, the procedure is independent of the modeling techniques used which allow direct comparisons across models made. The correlations of the standard predictions (i.e. fitted values) were compared to predictions where the predictor of interest has been randomly permutated. High correlation (i.e. the two predictions show little difference) indicates that the predictor permutated is not considered important for the model. Each of the predictors is then ranked based on the correlation coefficients and the proportion of the relative influence is scaled from zero to one. Hence, the higher the variable importance the more influential the predictor is in the model (Thuiller *et al.*, 2009).

Results

The mean $AUC_{evaluation}$ of the four ESPs climate-only models varied from 0.81 (cryoturbation) to 0.90 (palsa mires), whereas the corresponding TSS values varied from 0.51 (cryoturbation) to 0.87 (palsa mires). AUC and TSS values for slope processes (0.85 and 0.57) and nivation (0.82 and 0.56) were relatively similar. The inclusion of topography and soil variables significantly improved the transferability of the models (compared to climate-only models) for three ESPs (excluding cryoturbation) by both AUC and TSS values ($p \leq 0.05$) (Figures 5A, 5B, and 6). Because of the high correlation between the AUC and TSS values ($R = 0.95$, $p \leq 0.001$), only AUC results are shown hereafter. The evaluation statistics (mean $AUC_{evaluation}$) of the full models ranged from moderate (0.83, cryoturbation) to excellent (0.96, palsa mires). Similarly, AUC for slope processes and nivation were 0.91 and 0.88, respectively. The influence of the vegetation predictors on the climate–topography–soil models was relatively minor, mainly increasing the deviations among the modeling techniques rather than improving the predictions. A table showing the results from all of the modeling methods and model fitting-steps is provided as Supplementary Material Appendix B.

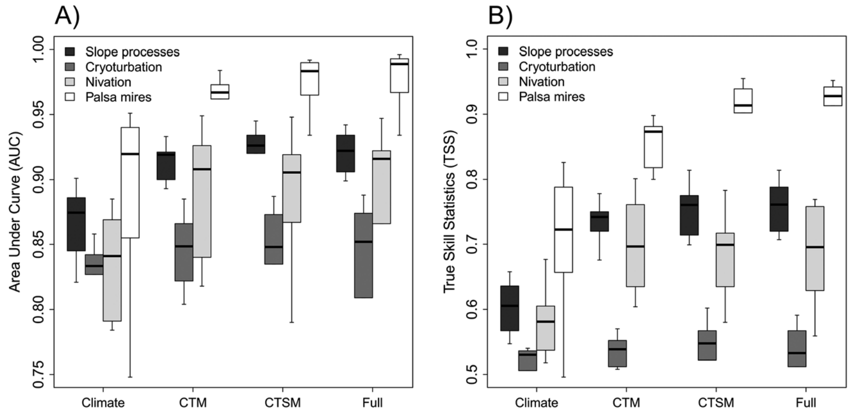

Figure 5. The improvement in evaluation statistics (i.e. the average of cross-validation rounds) along the model fitting-steps: (A) area under curve ($AUC_{evaluation}$) and, (B) true skill statistics ($TSS_{evaluation}$). Climate = climate variables only, CTM = climate and topography, CTSM = climate, topography and soil model, Full = full model (i.e. climate, topography, soil and vegetation variables included). The boxplots and whiskers show the variation across the 10 modeling techniques utilized (box represents median, first and third quartiles; the whiskers show the interquartile range × 1.5). Outliers are not shown for clarity.

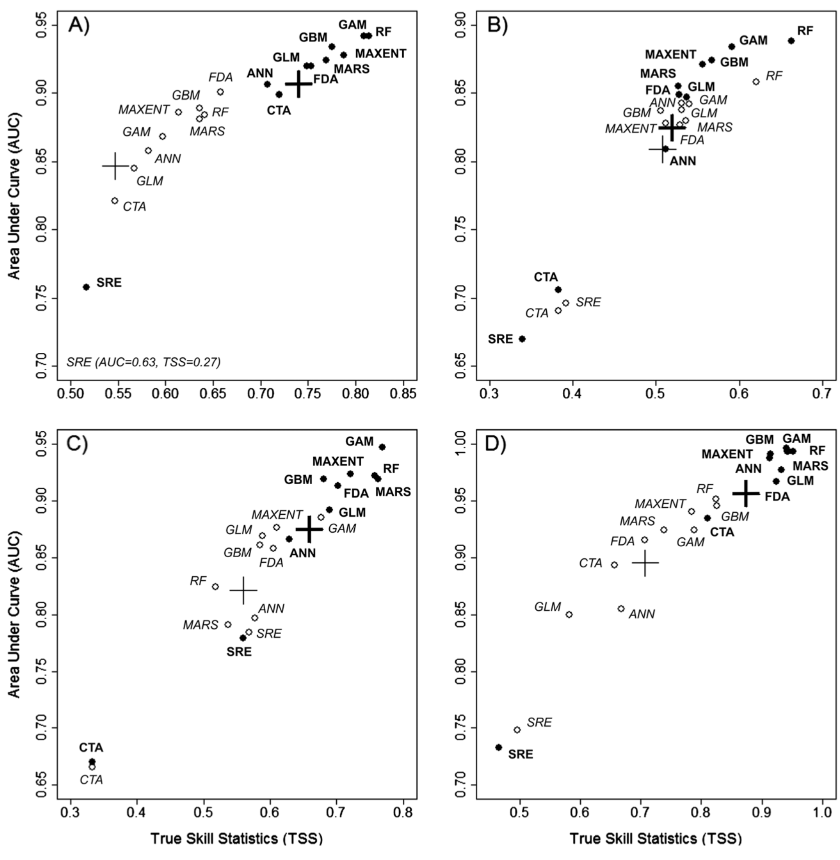

Figure 6. The performance of the modeling techniques respective of their average transferability (area under curve, $AUC_{evaluation}$ and true skill statistics, $TSS_{evaluation}$). (A) Slope processes, (B) cryoturbation, (C) nivation and (D) palsa mires. The empty circles refer to climate-only models and black circles to full models (i.e. climate, topography, soil and vegetation variables included). Similarly, thin crosses refer to the average of climate-only models and bold crosses show the average of full models.

Some significant correlations among the predictors exists (Supplementary Material Appendix C), for example, many of the climatological predictors were linked with each other (e.g. mean annual temperature and thawing degree days $R = 0.92$, $p \leq 0.001$) whereas, the correlation between the local predictors were lower (except the cover of peat and the cover of rock showed strong negative correlation; $R = -0.72$, $p \leq 0.001$). According to the variable importance calculated for the full models (averaged over all modeling techniques) the impact of climate predictors is pronounced for all of the response variables despite high deviations between the modeling techniques (Figure 7). Additionally, the explanatory analysis (Table II) and response curves estimated by GBMs (Figure 8; Supplementary Material Appendices D–F) are generally

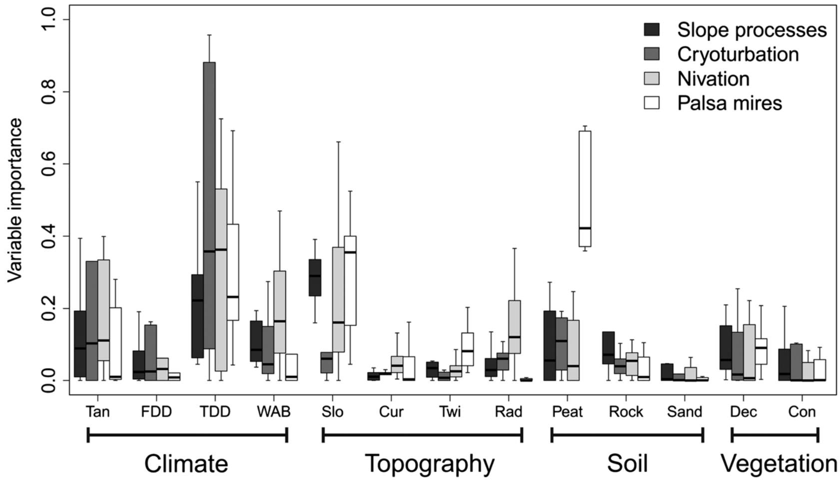

Figure 7. The variable importance of the full ESP models (i.e. climate, topography, soil and vegetation variables included). Tan = mean annual temperature, FDD = freezing degree days, TDD = thawing degree days, WAB = water balance, Slo = slope angle, Cur = curvature, TWI = topographic wetness index, Rad = radiation, Dec = cover of deciduous forest, Con = cover of coniferous forest. The boxplots and whiskers show the variation across the 10 modeling techniques utilized (box represents median, first and third quartiles; the whiskers show the interquartile range × 1.5). Outliers are not shown for clarity.

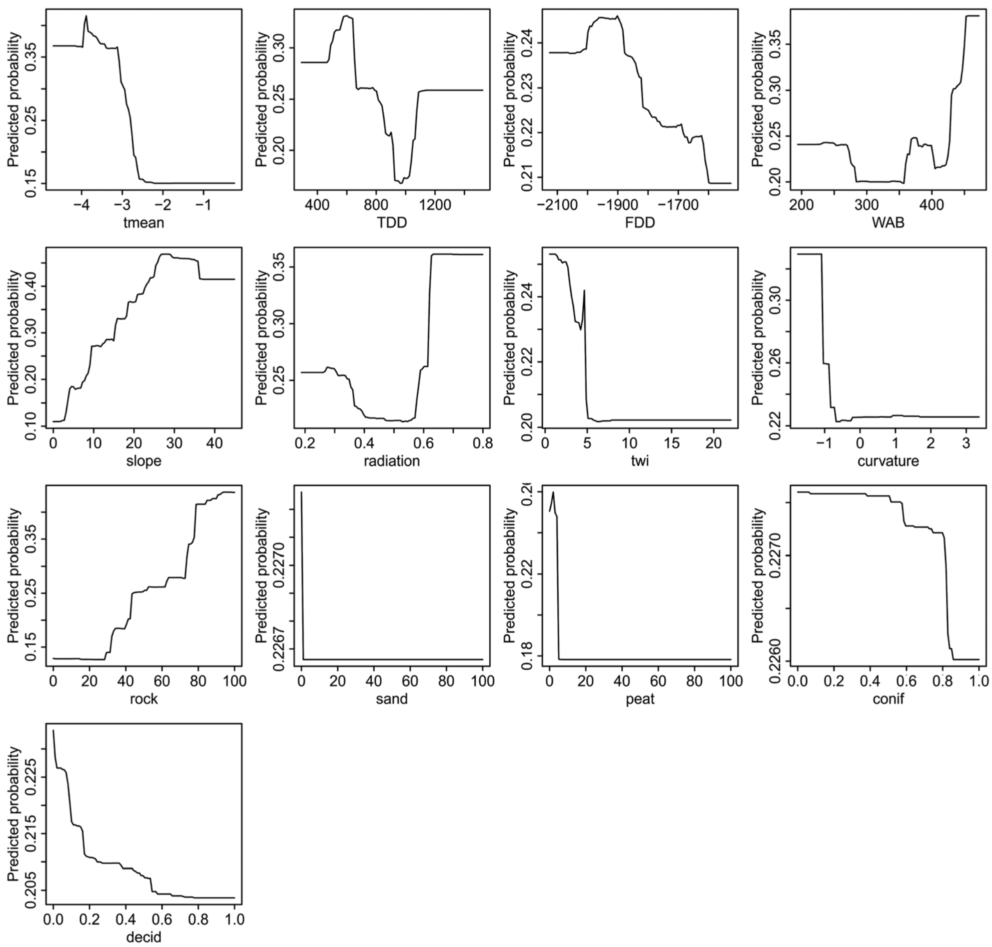

Figure 8. Response curves for full slope process models estimated by generalized boosting method (GBM).

consistent with the variable importance results. Slope processes are strongly associated with both climatic and topographic factors: the median importance of slope angle = 0.29 and TDD = 0.22 (Figures 7 and 8). For nivation the highest contribution derives from TDD (0.36) and slope angle (0.21). The probability of occurrence for both slope processes and nivation decreases with higher mean temperature while increasing with water balance and slope angle (Supplementary Material Appendix D). Similarly, cryoturbation is negatively linked to summer temperature with TDD (0.40) having the highest relative importance. Moreover, the response curves showed negative effect for slope angle and potential annual solar radiation suggesting that cryoturbation is more prevalent at the north-facing slopes on a relatively even terrain (Supplementary Material Appendix E). The occurrence of palsa mires is strongly associated with local soil and topography factors such as peat cover (0.42; positive effect) and slope angle (0.36; negative effect) with TDD also showing high relative importance (TDD = 0.23) with generally negative influence indicating that palsa mires are absent in the areas with TDD higher than 1200 °C (Supplementary Material Appendix F).

The compiled ensemble predictions (based on the *majoritys' vote* approach) across the study area are visualized in Figure 9 and in the Supplementary Material Appendices G–I. These prediction maps demonstrate how the spatial patterns of ESPs became more detailed and patchy as the additional local predictors were added to the climate-only models.

Discussion

Our results provide support for the argument that integrating both climate and local environmental information improves the predictions of ESPs in high latitudes. We show that with

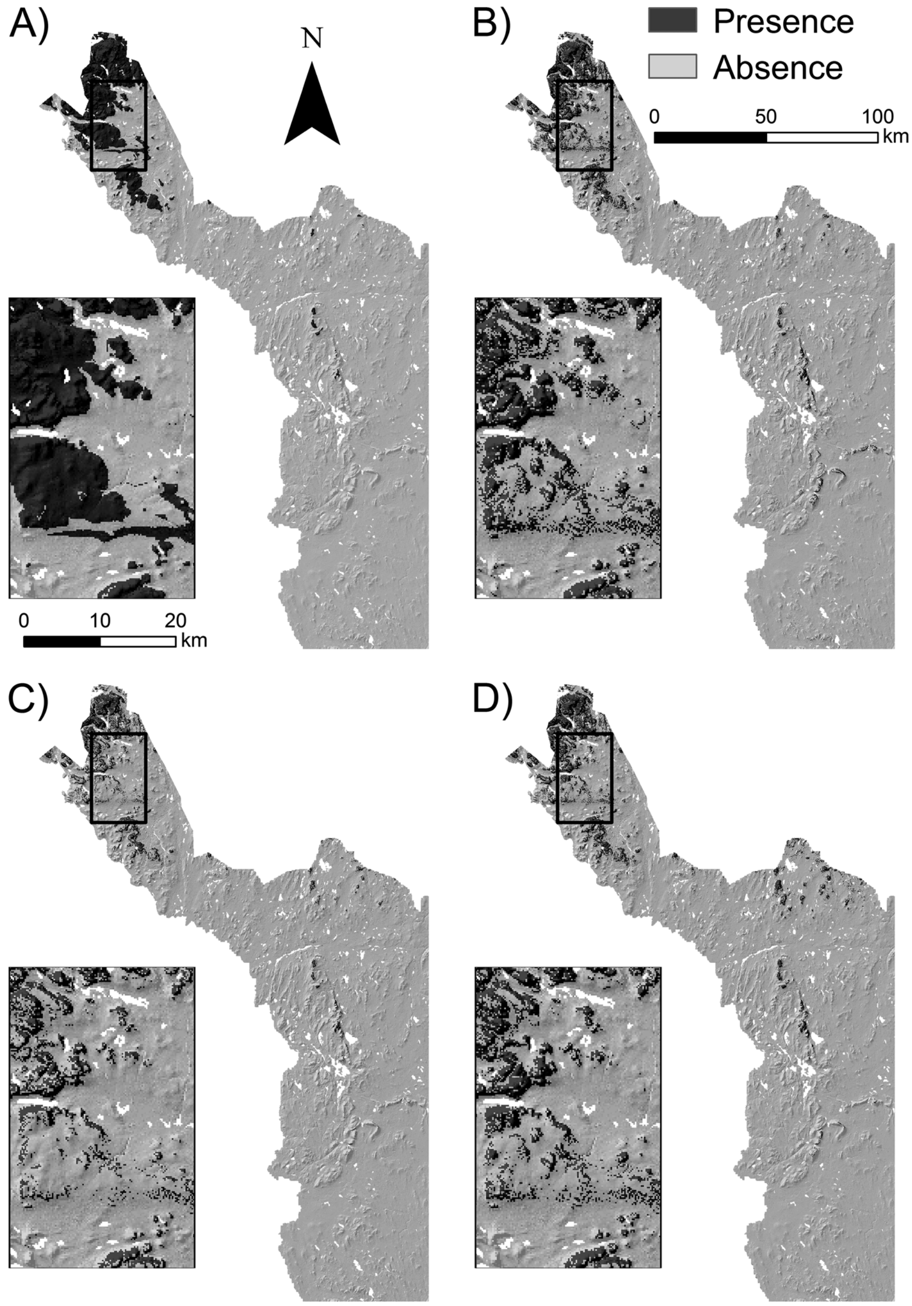

Figure 9. The predicted occurrence of slope processes along the model fitting-steps based on the *majoritys' vote* approach (see text for details) across the study area at the spatial resolution of 200 m × 200 m. (A) Climate-only; (B) climate and topography; (C) climate, topography and soil; (D) climate, topography, soil and vegetation.

models comprising solely of modeled climate predictors, the distribution of ESPs can be predicted with high accuracy. The inclusion of topography and soil predictors further improves the transferability of models for the four studied ESPs. Consequently, this study thus highlights the importance of incorporating climate and local predictors into GDMs at the landscape level.

The strong contribution of climate predictors is supported by both the model evaluation statistics and the variable importance results. Overall, the climate predictors turn out to be the most influential factors for almost all ESPs studied. Not surprisingly, palsa mires were the most accurately predicted, as the correlation between the climatological predictors and the distribution of permafrost is known to be strong (Sollid and Sørbel, 1998; Fronzek *et al.*, 2006; Etzelmüller *et al.*, 2011). The empirical relationships found in this study (in agreement with Luoto *et al.*, 2004) suggests that palsa mires are present at areas with low mean temperature conditions and relatively low precipitation (TDD < 1200 °C; TMEAN < -1.5 °C; WAB < 200 mm). The role of local factors such as soil and topography is evident: palsa mires are expected to occur at peaty lowlands (slope angle < 3°) where moisture is accumulated from the surrounding higher elevation areas and peat formations are generally developed (as suggested by the positive effect of TWI and peat cover) (Hjort *et al.*, 2007). Low temperature conditions combined with thin snow cover (i.e. open mires are exposed to strong winds redistributing the snow) allow deep frost penetration inside the moist peat layers and the initialization of the growth of palsa mounds (Seppälä, 1986; French, 2007).

On the contrary, cryoturbation models had the lowest transferability of the modeled ESPs. Moreover, the inclusion of local predictors to climate-only models had minor effects on cross-validation results of the cryoturbation models. The analysis revealed the importance of climate predictors mainly linked to diurnal, seasonal or permafrost derived freeze–thaw cycles in the topmost soil layers (Washburn, 1979; French, 2007). The most suitable climatological envelopes for cryoturbation are low temperature conditions (TMEAN < –2.5 °C and TDD < 700 °C) generally associated with mountain tops and valley bottoms with notable moisture surplus (WAB > 350 mm). These local climates increase soil wetness and together with sub-zero temperatures enables the frost to develop and operate effectively (Washburn, 1979; Haugland, 2004). In addition to these broader scale patterns, the response curves indicates active cryoturbation occurrence at relatively low slope angles (< 5°) and/or areas with low radiation conditions (intense frost activity). The negative relationship between cryoturbation and slope angle contradicts the explanatory analysis, which associates the cryoturbated soils with higher inclinations. However, Luoto and Hjort (2005) suggest that some of the cryoturbation forms (i.e. sorted patterned ground) are defined with relative high slope angle, while non-sorted patterned ground and earth hummocks are more common on wetter valley bottoms (concave terrain) with silty till and peat soils, respectively. Additionally, the independent contribution of the topographical wetness index was surprisingly low, contradicting the known relationship between cryoturbation and soil moisture previously demonstrated by Matthews *et al.* (1998) as well as Hjort and Luoto (2010). This discrepancy is possibly due to fundamental problems related to DEM-derived indices as topographic wetness index has recently been shown to be weakly linked to observed soil moisture in high-latitude environments (le Roux *et al.*, 2013a).

Our results (in agreement with Christiansen, 1998) suggest that the occurrence of slope processes and nivation are strongly modified by local topography and climate. Furthermore, the distribution of nivation is mainly controlled by the amount of snow rainfall (WAB > 400 mm), the duration of melting period (TDD < 500 °C) and mean annual temperature (TMEAN < −2.5 °C). In addition, the nivation sites are likely to occur at topographically complex areas characterized by low incoming solar radiation and sheltered conditions against strong winds redistributing snow (i.e. high slope angles with north-facing aspect and concave terrain). These topographically heterogeneous sites promote the formation and persistence of the snow packs across the seasons (Kivinen *et al.*, 2012). Similarly, we also show (in consensus with Matsuoka, 2005) that slow slope processes (i.e. solifluction) at high latitudes are mainly dependent on topographical and climatological factors. At the broader scale the role of climatic predictors is pronounced; the occurrence of slope processes is strongly controlled by mean annual temperatures conditions (TMEAN < –2.5 °C) creating conditions favorable to seasonal and permafrost formation (French, 2007). Not surprisingly, the single most important predictor was slope angle, which is related to the potential energy and drainage patterns of the hill slope (Washburn, 1979; Moore *et al.*, 1991). Our results (in consensus with Matsuoka, 2001) indicate strong positive correlation between slope processes and slope angle suggesting the initiation of the downward soil movement at very low inclinations (slope angle > 3°). As the physical mechanisms of slope processes at high latitudes are diverse (Washburn, 1979; Matsuoka, 2005; French, 2007), different factors drive the activity of these processes. The low mean temperatures (TMEAN and FDD) are more linked to the seasonal frost activity; thus the slope adjustment is related to vertical heaving and downward settling of the soil surface (i.e. frost creep) (Matsuoka, 2005). The increased thaw-period temperatures (TDD) and soil wetness in turn promote the movement of thawing active layer against permafrost table (i.e. gelifluction) (Harris *et al.*, 2001). Interestingly, the effects of the vegetation variables were modest for all of the response variables, increasing the deviations among the modeling techniques rather than improving the predictions. This may be due to the fact that at this spatial scale other factors overcome the potential effects of vegetation, which (due to for example stabilizing the soil surface and affecting hydrological properties of the soil) are potentially more apparent at finer spatial scales (Viles *et al.*, 2008; Malanson *et al.*, 2012).

The 10 modeling techniques utilized in this study produced notable variations across the evaluations statistics resulting from different statistical approaches (Thuiller *et al.*, 2013). Even though most of the machine learning and classification methods (RF, GBM, MAXENT and FDA) performed well in terms of model transferability (in agreement with Hjort and Marmion, 2009; Heikkinen *et al.* 2012; Hjort *et al.*, 2013), other sophisticated techniques (e.g. ANN) showed only moderate performance. From the regression-based methods, GAM had high modeling capability while others (GLM and MARS) had more intermediate prediction accuracy. More precisely, in our study the RF and GAM turn out to be the most reliable and consistent methods. These techniques produced repeatedly the most accurate predictions across the cross-validation statistics, thus supporting their applicability to predict geomorphic systems (in agreement with Brenning *et al.*, 2007; Marmion *et al.*, 2008; Hjort and Luoto, 2010). In general, SRE and CTA were the weakest techniques utilized providing consistently the least accurate predictions. These findings agree with earlier studies showing that CTA often produce overly complex models with the expense of transferability (Luoto and Hjort, 2005; Marmion *et al.*, 2008). Additionally, this study demonstrates the over simplistic nature of range-based technique SRE, thus failing to capture the potentially complex ESP–environment relationships, at least in landscape scale analysis. The applied model ensemble approach provided a useful framework to account for the methodological differences, as the results are not sensitive to the choice of a single modeling technique (Araújo and New, 2006; Marmion *et al.*, 2009; Luoto *et al.*, 2010). Further, this methodology enhances the reliability of the forecasts in geomorphology as it combines the model outputs of different algorithms (e.g. regression, classification trees and machine learning) into a single binary agreement map (Gallien *et al.*, 2012). The fitted models showed high levels of complexity (the number of environmental gradients) and some significant pairwise correlations among the predictors. However, in this predictive modeling context the best results are achieved by incorporating all climate and local predictors simultaneously as opposed to selecting a single inter-correlated variable (e.g. mean temperature) representing all the climatological gradients (Braunisch *et al.*, 2013).

Geomorphic process–environment relationships can be addressed via a hierarchical modeling framework (see Pearson and Dawson, 2003) where various factors operate at different spatial scales and suitable environmental envelopes for ESPs are narrowed with every step down the hierarchy. Thus, at the broad scale (continental–regional), climate can be considered as the dominant factor determining the coarse-grained distribution of ESPs. However, at finer scales (landscape–local) predictors such as topography and soil become more relevant and the distribution patterns of ESPs become increasingly detailed and patchy. In this study, the compiled ensemble prediction maps reflect the increase in local variability inside suitable climatic envelope, determining the optimal environmental conditions favorable for the occurrence of ESPs. Since the distribution of the key ESPs under current climate can now accurately be modeled, it is important to proceed to investigate how these processes may evolve under warmer future climates (e.g. Etzelmüller, 2013). The potential changes of ESP activity in these systems might feedback e.g. through changes in vegetation and carbon cycle with possible global implications (Christensen *et al.*, 2004; Knight and Harrison, 2012; Elberling *et al.*, 2013).

Conclusions

This study emphasizes the demand for accurate climate data for use in predictive geomorphological mapping in high-latitude regions. Nonetheless, the models of ESPs will benefit from the inclusion of local predictors with higher transferability compared to climate-only models. In summary, our results have both theoretical and applied importance. First, we identified the main environmental factors controlling the distribution of the four key ESPs at high-latitudes. Second, by utilizing the recent developments in spatial modeling techniques and accurate environmental predictors, we created realistic estimates of the distribution of ESPs across large environmental gradients. By determining the most influential factors of multiple ESPs, we will be able to project their dynamics in response to changes in climate and identify processes that are particularly sensitive to forecasted climate change. Furthermore, the modeling outputs of this study can serve as a valuable data source for other studies (e.g. global change impact models) in the investigated high-latitude regions.

Acknowledgements—JA was funded by the Geography Graduate School of the Academy of Finland. ML acknowledges funding from the Academy of Finland (Project Number 1140873). The authors thank Annina Niskanen for improving the English of the manuscript and two anonymous reviewers for their constructive comments.

References

Aalto J, le Roux PC, Luoto M. 2014. The meso-scale drivers of temperature extremes in high-latitude Fennoscandia. *Climate Dynamics* **42**: 237–252.

Albrecht J, Car A. 1999. GIS analysis for scale-sensitive environment modelling based on hierarchy theory. In *GIS for Earth Surface Systems*, Dikau R, Saurer H (eds). Gebrüder Borntraeger: Berlin; 1–23.

Allouche O, Tsoar A, Kadmon R. 2006. Assessing the accuracy of species distribution models: prevalence, kappa and the true skill statistic (TSS). *Journal of Applied Ecology* **43**: 1223–1232.

Araújo MB, New M. 2006. Ensemble forecasting of species distributions. *TRENDS in Ecology and Evolution* **22**: 42–47.

Ballantyne CK, Benn DI. 1994. Paraglacial slope adjustement and resedimentation following recent glacier retreat, Fåberstølsdalen, Norway. *Arctic and Alpine Research* **26**: 255–269.

Beamount LJ, Hughes L, Poulsen M. 2005. Predicting species distributions: use of climatic parameters in BIOCLIM and its impact on predictions of species' current and future distributions. *Ecological Modelling* **186**: 250–269.

Beven K, Kirkby M. 1979. A physically based variable contributing area model of basin hydrology. *Hydrological Sciences Bulletin* **24**: 43–69.

Braunisch V, Coppes J, Arlettaz R, Suchant R, Schmid H, Bollman K. 2013. Selecting from correlated climate variables: a major source of uncertainty for predicting species distributions under climate change. *Ecography* **36**: 1–13.

Breiman L. 2001. Random forests. *Machine Learning* **45**: 5–32.

Breiman L, Friedman F, Olshen F, Stone C. 1984. Classification and regression trees. In *Wadsworth Statistics/Probability Series*. Wadsworth: Belmont, CA; 358 pp.

Brenning A, Azócar GF. 2010. Statistical analysis of topographic and climatic controls and multispectral signatures of rock glaciers in the dry Andes, Chile (27°–33°S). *Permafrost and Periglacial Processes* **21**: 54–66.

Brenning A, Grasser M, Friend DA. 2007. Statistical estimation and generalized additive modeling of rock glacier distribution in the San Juan Mountains, Colorado, United States. *Journal of Geophysical Research* **112**: F02S15. DOI.10.1029/2006JF000528

Burnett MR, August PV, Brown JH, Killingbeck KT. 1998. The influence of geomorphological heterogeneity on biodiversity: I. A patch scale perspective. *Conservation Biology* **12**: 363–370.

Carter TR, Porter JH, Parry ML. 1991. Climatic warming and crop potential in Europe: prospects and uncertainties. *Global Environmental Change* **1**: 291–312.

Christiansen HH. 1998. Nivation forms and processes in unconsolidated sediments, NE Greenland. *Earth Surface Processes and Landforms* **23**: 751–760.

Christensen TR, Johansson T, Åkerman HJ, Mastepanov M, Friborg T, Crill P, Svensson BH. 2004. Thawing sub-arctic permafrost: effects on vegetation and methane emissions. *Geophysical Research Letters* **31**: L04501. DOI. 10.1029/2003GL018680

Dai FC, Lee CF. 2002. Landslide characteristics and slope instability modelling using GIS, Lantau Island, Hong Kong. *Geomorphology* **42**: 213–228.

Elberling B, Michelsen A, Schädel C, Schuur EAG, Christiansen HH, Berg L, Tamstorf MP, Sigsgaard C. 2013. Long-term CO_2 production following permafrost thaw. *Nature Climate Change* **3**: 890–894.

Elith J, Leathwick JR, Hastie T. 2008. A working guide to boosted regression trees. *Journal of Animal Ecology* **77**: 802–813.

Esri. 2013. ArcScripts. www.arcsripts.esri.com [25 September 2013].

Etzelmüller B. 2013. Recent advances in mountain permafrost research. *Permafrost and Periglacial Processes* **24**: 99–107. DOI. 10.1002/ppp.1772

Etzelmüller B, Schuler TV, Isaksen K, Christiansen HH, Farbrot H, Benestad R. 2011. Modelling the temperature evolution of Svalbard permafrost during the 20th and 21st century. *The Cryosphere* **5**: 67–79.

Farbrot H, Isaksen K, Etzelmüller B, Gisnås K. 2013. Ground thermal regime and permafrost distribution under a changing climate in northern Norway. *Permafrost and Periglacial Processes* **24**: 20–38.

Fielding AH, Bell JF. 1997. A review of methods for the assessment of prediction errors in conservation presence/absence models. *Environmental Conservation* **24**: 38–49.

Finnish Environmental Institute. 2006. Corine Land Cover 2006. http://wwwd3.ymparisto.fi/d3/Static_rs/spesific/corinelandcover.html [28 January 2014].

Fox JF. 1981. Intermediate levels of soil disturbance maximize alpine plant diversity. *Nature* **293**: 564–565.

French HM. 2007. *The Periglacial Environment*. John Wiley & Sons: Chichester.

Friedman J. 1991. Multivariate adaptive regression splines. *Annals of Statistics* **19**: 1–141.

Fronzek S, Carter TR, Luoto M. 2011. Evaluating sources of uncertainty in modeling the impact of probabilistic climate change on sub-arctic palsa mires. *Natural Hazards and Earth System Sciences* **11**: 2981–2995.

Fronzek S, Luoto M, Carter TR. 2006. Potential effect of climate change on the distribution of palsa mires in subarctic Fennoscandia. *Climate Research* **32**: 1–12.

Gallien L, Douzet R, Pratte S, Zimmermann NE, Thuiller W. 2012. Invasive species distribution models – how violating the equilibrium assumption can create new insights. *Global Ecology and Biogeography* **21**: 1126–1136.

Geological Survey of Finland. 2010. *Digital Soil Database*. Geological Survey of Finland: Espoo.

Goetz JN, Brenning A, Guthrie RH. 2012. Exploring regional topographic and rainfall controls of landslides on Vancouver Island, British Columbia, Canada. In *Landslides and Engineered Slopes: Protecting Society through Improved Understanding. Proceedings of the 11th International and 2nd North American Symposium on Landslides and Engineered Slopes, Banff, Canada, 3–8 June 2012*. Eberhardt E, Froese C, Turner AK, Leroueil S (eds). CRC Press/ Balkema: Leiden; vol. **1**, 429–435.

Guisan A, Zimmermann NE. 2000. Predictive habitat distribution models in ecology. *Ecological Modelling* **135**: 147–186.

Harris C, Rea B, Davies M. 2001. Scaled physical modelling of mass movement process on thawing slopes. *Permafrost and Periglacial Processes* **12**: 125–135.

Harris C, Smith JS, Davies MCR, Rea B. 2008. An investigation of periglacial slope stability in relation to soil properties based on physical modelling in the geotechnical centrifuge. *Geomorphology* **93**: 437–459.

Hastie T, Tibshirani R. 1990. Generalized additive models. In *Monographs on Statistics and Applied Probability 43*. Chapman and Hall: New York.

Hastie T, Tibshirani R, Buja A. 1994. Flexible discriminant analysis by optimal scoring. *Journal of the American Statistical Association* **89**: 1255–1270.

Haugland JE. 2004. Formation of patterned ground and fine–scale soil development within two late Holocene glacial chronosequences: Joutunheimen, Norway. *Geomorphology* **61**: 287–301.

Heikkinen RK, Marmion M, Luoto M. 2012. Does the interpolation accuracy of species distribution models come at the expense of transferability? *Ecography* **35**: 276–288.

Hjort J, Etzelmüller B, Tolgensbakk J. 2010. Effects of scale and data source in periglacial distribution modelling in a high arctic environment, western Svalbard. *Permafrost and Periglacial Processes* **21**: 345–354.

Hjort J, Luoto M. 2008. Can abundance of geomorphological features be predicted using presence–absence data? *Earth Surface Processes and Landforms* **33**: 741–750.

Hjort J, Luoto M. 2009. Interaction of geomorphic and ecologic features across altitudinal zones in a subarctic landscape. *Geomorphology* **112**: 324–333.

Hjort J, Luoto M. 2010. Novel theoretical insights into geomorphic process–environment relationship using simulated response curves. *Earth Surface Processes and Landforms* **35**: 363–371.

Hjort J, Luoto M. 2013. Statistical methods for geomorphic distribution modeling. In *Treatise on Geomorphology*, Scroder JF (ed). Elsevier: San Diego, CA; 59–73.

Hjort J, Luoto M, Seppälä M. 2007. Landscape scale determinants of periglacial features in subarctic Finland: a grid-based modelling approach. *Permafrost and Periglacial Processes* **18**: 115–127.

Hjort J, Marmion M. 2009. Periglacial distribution modelling with a boosting method. *Permafrost and Periglacial Processes* **20**: 15–25.

Hjort J, Ujanen J, Parviainen M, Tolgensbakk J, Etzelmüller B. 2013. Transferability of geomorphological distribution models: evaluation using solifluction features in subarctic and Arctic regions. *Geomorphology* **204**: 165–176.

Intergovernmental Panel on Climate Change (IPCC). 2007. Polar regions (Arctic and Antarctic). In *Climate Change 2007: Impacts, Adaptation and Vulnerability. Contribution of Working Group II to the Fourth Assessment Report of the Intergovernmental Panel on Climate Change*. Parry ML, Canziani OL, Palutikof JP, Van der Linden PJ, Hanson CE (eds). Cambridge University Press: Cambridge; 653–685.

Kivinen S, Kaarlejärvi E, Jylhä K, Räisänen J. 2012. Spatiotemporal distribution of threatened high-latitude snowbed and snow patch habitats in warming climate. *Environmental Research Letters* **7**: 034024. DOI. 10.1088/1748-9326/7/3/034024

Knight J, Harrison S. 2012. The impacts of climate change on terrestrial Earth surface systems. *Nature Climate Change* **3**: 24–29. DOI. 10.1038/NCLIMATE1660

Laitakari I. 1998. Peruskallion myöhäiset kehitysvaiheet – miljardi rauhallista vuotta. In *Suomen kallioperä – 3000 vuosimiljoonaa*, Lehtinen M, Nurmi P, Rämö T (eds). Suomen geologinen seura: Helsinki (in Finnish).

Land Survey of Finland. 2013. MapSite. http://kansalaisen.karttapaikka.fi/kartanhaku/osoitehaku [19 September 2013].

Luoto M, Fronzek S, Zuidhoff FS. 2004. Spatial modeling of palsa mires in relation to climate in northern Europe. *Earth Surface Processes and Landforms* **29**: 1373–1387.

Luoto M, Hjort J. 2004. Generalized linear modelling in periglacial studies: terrain parameters and patterned ground. *Permafrost and Periglacial Processes* **15**: 327–338.

Luoto M, Hjort J. 2005. Evaluation of current statistical approaches for predictive geomorphological mapping. *Geomorphology* **67**: 299–315.

Luoto M, Marmion M, Hjort J. 2010. Assessing spatial uncertainty in predictive geomorphological mapping: a multi-modelling approach. *Computer & Geosciences* **36**: 355–361.

Luoto M, Seppälä M. 2002. Modelling the distribution of palsas in Finnish Lapland with logistic regression and GIS. *Permafrost and Periglacial Processes* **13**: 17–28.

Malanson GP, Bengtson LE, Fagrem DB. 2012. Geomorphic determinants of species composition of alpine tundra, Glacier national park, U.S.A. *Arctic, Antartic, and Alpine Research* **44**: 197–209.

Marmion M, Hjort J, Thuiller W, Luoto M. 2008. A comparison of predictive methods in modelling the distribution of periglacial landforms in Finnish Lapland. *Earth Surface Processes and Landforms* **33**: 2241–2254.

Marmion M, Hjort J, Thuiller W, Luoto M. 2009. Statistical consensus methods for improving predictive geomorphology maps. *Computer and Geosciences* **35**: 615–625.

Matthews JA, Shakesby RA, Berrisfjord MS, McEwen LJ. 1998. Periglacial patterned ground on the Styggedalsbreen glacier foreland, Jotunheimen, southern Norway: micro-topographic, paraglacial and geoecological controls. *Permafrost and Periglacial Processes* **9**: 147–166.

Matsuoka N.. 2001. Solifluction rates, processes and landforms: a global review. *Earth-Science Reviews* **55**: 107–134.

Matsuoka N. 2005. Temporal and spatial variations in periglacial soil movements on alpine crest slopes. *Earth Surface Processes and Landforms* **30**: 41–58.

McCullagh P, Nelder JA. 1989. *Generalized Linear Models*, 2nd edn. Chapman & Hall: New York; 511 pp.

McCune B, Keon D. 2002. Equations for potential annual direct incident radiation and heat load. *Journal of Vegetation Science* **13**: 603–606.

Moore ID, Grayson RB, Ladson AR. 1991. Digital terrain modelling: a review of hydrological, geomorphological, and biological applications. *Hydrological Processes* **5**: 3–30.

Pearson RG, Dawson TP. 2003. Predicting the impacts of climate change on the distribution of species: are bioclimate envelope models useful? *Global Ecology and Biogeography* **12**: 361–371.

Phillips JD. 2003. Sources of nonlinearity and complexity in geomorphic systems. *Progress in Physical Geography* **27**: 1–23.

Phillips SJ, Anderson RP, Schapire RE. 2006. Maximum entropy modelling of species geographic distributions. *Ecological Modelling* **190**: 231–259.

Potter KA. 2013. Microclimatic challenges in global change biology. *Global Change Biology* **19**: 2932–2939. DOI. 10.1111/gcb.12257

R Development Core Team. 2011. R: A language and environment for statistical computing. R Foundation for Statistical Computing: Vienna. http://www.R-project.org/

Ridefelt H, Etzelmüller B, Boelhouwers J. 2010. Spatial analysis of solifluction landforms and process rates in the Abisko Mountains, northern Sweden. *Permafrost and Periglacial Processes* **21**: 241–255.
le Roux PC, Aalto J, Luoto M. 2013a. Soil moisture's underestimated role in climate change impact modelling in low-energy systems. *Global Change Biology* **19**: 2965–2975. DOI. 10.1111/gcb.12286
le Roux PC, Luoto M. 2014. Earth surface processes drive the richness, composition and occurrence of plant species in an arctic-alpine environment. *Journal of Vegetation Science* **25**: 45–54. DOI. 0.1111/jvs.12059
le Roux PC, Virtanen R, Luoto M. 2013b. Geomorphological disturbance is necessary for predicting fine-scale species distributions. *Ecography* **36**: 800–808.
Schumm SA. 1979. Geomorphic thresholds: the concept and its applications. *Transactions of the Institute of British Geographers, New Series* **4**: 485–515.
Seppälä M. 1986. The origin of palsas. *Geografiska Annaler* **68A**: 141–147.
Seppälä M. 1988. Palsas and related forms. In *Advances in Periglacial Geomorphology*, Clark M (ed.). John Wiley & Sons: Chichester; 247–278.
Seppälä M. 2005. Frost heave on earth hummocks (pounus) in Finnish Lapland. *Norsk Geografisk Tidsskrift – Norwegian Journal of Geography* **59**: 171–176.
Skov F, Svenning JC. 2004. Potential impacts of climatic change on the distribution of forest herbs in Europe. *Ecography* **27**: 366–380.
Sollid JL, Sørbel L. 1998. Palsa bogs as a climate indicator: examples from Dovrefjell, southern Norway. *Ambio* **27**: 287–291.
Sormunen H, Virtanen R, Luoto M. 2010. Inclusion of local environmental conditions alters high-latitude vegetation change predictions based on bioclimatic models. *Polar Biology* **34**: 883–897.
Swets K. 1988. Measuring the accuracy of diagnostic systems. *Science* **240**: 1285–1293.
Tarnocai C, Canadell JG, Schuur EAG, Kuhry P, Mazhitova G, Zimow S. 2009. Soil organic carbon pools in the northern circumpolar permafrost region. *Global Biogeochemical Cycles* **23**: GB2023. DOI. 10.1029/2008GB003327
Thorn C. 1979. Ground temperatures and surficial transport in colluvium during snowpatch meltout; Colorado front range. *Arctic and Alpine Research* **11**: 41–52.
Thuiller W, Georges D, Engler R. 2013. biomod2: Ensemble platform for species distribution modeling. R package version 2.1.15. http://CRAN.R-project.org/package=biomod2
Thuiller W, Lafourcade B, Engler R, Araújo MB. 2009. BIOMOD – a platform for ensemble forecasting of species distributions. *Ecography* **32**: 369–373.
Venables WN, Ripley BD. 2002. *Modern Applied Statistics with S*, 4th edn. Springer: Berlin; 495 pp.
Viles HA, Naylor LA, Carter NEA, Chaput D. 2008. Biogeomorphological disturbance regimes: progress in linking ecological and geomorphological systems. *Earth Surface Processes and Landforms* **33**: 1419–1435.
Virtanen R, Luoto M, Rämä T, Mikkola K, Hjort J, Grytnes JA, Birks JB. 2010. Recent vegetation changes at the high-latitude tree line ecotone are controlled by geomorphological disturbance, productivity and diversity. *Global Ecology and Biogeography* **19**: 810–821.
Walker MD. 1995. Patterns and causes of Arctic plant community diversity. In *Arctic and Alpine Biodiversity*, Chapin FS III, Körner C (eds). Springer-Verlag: Berlin; 3–20.
Walsh SJ, Butler DR, Malanson GP. 1998. An overview of scale, pattern, process relationships in geomorphology: a remote sensing and GIS perspective. *Geomorphology* **21**: 183–205.
Washburn AL. 1979. *Geocryology – A Survey of Periglacial Processes and Environments*. Arnold: London.

Supporting Information

Additional supporting information may be found in the online version of this article at the publisher's web-site.

